

Multimedia on the Mountaintop: Using Public Snow Images to Improve Water Systems Operation

Andrea Castelletti, Roman Fedorov, Piero Fraternali, Matteo Giuliani
Politecnico di Milano, Dipartimento di Elettronica, Informazione e Bioingegneria, Milan, Italy
first.last@polimi.it

ABSTRACT

This paper merges multimedia and environmental research to verify the utility of public web images for improving water management in periods of water scarcity, an increasingly critical event due to climate change. A multimedia processing pipeline fetches mountain images from multiple sources and extracts virtual snow indexes correlated to the amount of water accumulated in the snow pack. Such indexes are used to predict water availability and design the operating policy of Lake Como, Italy. The performance of this informed policy is contrasted, via simulation, with the current operation, which depends only on lake water level and day of the year, and with a policy that exploits official Snow Water Equivalent (SWE) estimated from ground stations data and satellite imagery. Virtual snow indexes allow improving the system performance by 11.6% w.r.t. the baseline operation, and yield further improvement when coupled with official SWE information, showing that the two data sources are complementary. The proposed approach exemplifies the opportunities and challenges of applying multimedia content analysis methods to complex environmental problems.

CCS Concepts

- **Computing methodologies** → **Visual content-based indexing and retrieval**; Image segmentation; Matching;
- **Applied computing** → *Environmental sciences*;

Keywords

Image processing, crowdsourcing, snow, environment monitoring, water management

1. INTRODUCTION

Water scarcity resulting from climate change has entered the global agenda due to its impact on society and economy

This work was partially funded by the CHEST FP7 project of the European Commission.

Permission to make digital or hard copies of all or part of this work for personal or classroom use is granted without fee provided that copies are not made or distributed for profit or commercial advantage and that copies bear this notice and the full citation on the first page. Copyrights for components of this work owned by others than ACM must be honored. Abstracting with credit is permitted. To copy otherwise, or republish, to post on servers or to redistribute to lists, requires prior specific permission and/or a fee. Request permissions from permissions@acm.org.

MM '16, October 15-19, 2016, Amsterdam, Netherlands

© 2016 ACM. ISBN 978-1-4503-3603-1/16/10...\$15.00

DOI: <http://dx.doi.org/10.1145/2964284.2976759>

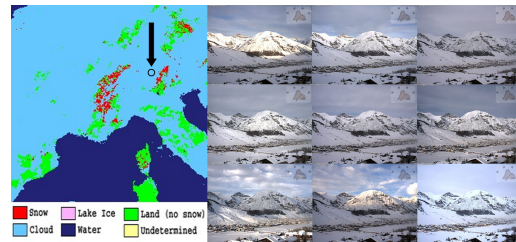


Figure 1: left: MODIS daily snow cover map on Jan. 9 2014; right: images acquired the same day by a webcam in the position shown by the black circle.

and is recognized as a global risk already in the short term [10]. Re-solving the uneven spatio-temporal distribution of water requires storing it when it is naturally available (e.g. when snow is melting) and delivering when required by users (e.g. agriculture, hydropower). Dam operators must hence balance the amount of water to release for short term needs with the amount to store for future demands, particularly during the dry season, possibly based on predicted water availability. The Snow Water Equivalent (SWE), i.e., the water content of the snow pack, is an important hydrological variable used to predict future water availability. State-of-practice SWE monitoring applications rely on mathematical models often based on physical laws, ad hoc campaigns, and dedicated observations from ground stations or remote sensing (specialized satellite products), which cannot be easily validated against ground truth given the high spatial heterogeneity of SWE and the few SWE point measurements available.

The public visual content generated by users or by low cost and widely available ground sensors, such as webcams, raises the question of whether it is possible to use such data, albeit collected for completely different purposes and with lower quality, as a replacement or complement to the high quality, but also more restricted and costly, data traditionally employed by environmental models, and specifically by water management models. Recently, as discussed in [2], various authors have shown the potential of using public content for monitoring natural processes [25], hazards [5], and more. However the claim that web media provides an effective input for environmental models, usable to deliver reliable management decisions, has still to be demonstrated. In this work, we build an automatic data processing architecture and apply it to investigate the operational value of public

web images, either produced by users or generated by touristic webcams, as an input to an environmental model; as a case study, we focus on a management problem that entails the daily water release decisions for a sub-alpine regulated lake. Traditionally, the decision of how much water to release, which influences the level of the lake, is taken in two ways: by a limited information policy considering only the current lake level and the day of the year; or by a more sophisticated policy relying on a hydrological predictive model of the future water availability, which exploits snow information (typically, SWE). In our case study, a SWE time series is estimated weekly by the Regional Environmental Protection Agency (ARPA) through a hybrid of satellite retrieved information, ground observation, and model outputs. Ground stations and satellite data, however, have limits when used to predict snow processes, which exhibit high spatio-temporal variability [7, 25]. Ground stations are few and coarsely distributed, especially in high altitude regions. Satellite snow products have limitations in alpine contexts [7]: space-board passive microwave radiometers (e.g., AMSR-E) penetrate clouds and provide accurate snow cover estimation, but have coarse spatial resolution (25 km); active microwave systems (e.g., RADARSAT) detect the presence of liquid water content, but require additional ground observations to make accurate estimates, whereas optical sensors (e.g., MODIS) generate high spatial and temporal resolution maps, yet cannot see the earth surface when clouds are present. As an example, Figure 1 shows how clouds can occlude the satellite view, but not the ground view: the left part shows the “MODIS/Terra Snow Cover Daily L3” snow map on Jan. 9, 2014, where most of the Alps area is covered by clouds and provides no snow information; the right part shows images taken the same day by a webcam placed in Livigno, Italy (its position is denoted by the black circle in the satellite map). High clouds prevent satellite snow estimation, but do not occlude the ground view, which gives complementary information.

The research question addressed in this paper is whether visual content acquired from the web can bring a quantifiable contribution as a replacement or supplement to traditional input for environmental models. The case study used to verify the hypothesis focuses on snow information for informing water system operation and exploits an architecture that automatically crawls content from multiple web data sources, retains only geo-tagged images containing a mountain skyline with high probability, identifies the visible peaks in each image using a public online digital terrain model, classifies the image pixels as snow or no-snow to obtain a *snow mask* per image, and, finally, extracts time series of *virtual snow indexes* usable as a proxy of the snow covered area. To assess the operational value of such indexes, a simulation is performed of alternative control policies that decide the daily operations (i.e., how much water to release) for Lake Como, based on different inputs. As a criterion for defining performance, a multi-objective tradeoff function is used, which pursues two competing objectives: avoiding floods on the lake shores due to excessive water storage and delivering sufficient water to the downstream agricultural districts. Several control policies are contrasted, and the results prove that virtual snow indexes improve the system performance, and can be combined with the official ARPA SWE data. Beside the specific impact in the snow monitoring and water management fields, the described approach can stimulate

a **whole new branch of public web media exploitation** in many environmental monitoring problems. Previous work has applied multimedia processing techniques to extract environment-related data from public media, but struggled to convince environmental scientists that such data are useful. This work demonstrates that it is possible to extract environment-related information from public media, automatically and at scale, and that the extracted data are improving the performance of an environmental model. Such deep integration between multimedia and environment research can have **radical impact on environment monitoring as done today, and on environmental and societal objectives at large**; this goal challenges multimedia research to measure the impact of data extraction techniques on the performance of practical environmental models, going beyond evaluation of mere algorithm accuracy.

The original contributions of the paper are:

- A web multimedia content processing pipeline that automatically extracts environmental meta-data from users’ mountain photos and touristic webcam streams. The pipeline employs a mountain image classifier (with 94% precision, 96.3% recall), a weather condition filter, with 87.4% True Positive Rate at 3.5% False Positive Rate, a peak detection algorithm (with 75% overall accuracy, 81% in good meteorological conditions) based on a matching procedure between an image and a virtual panorama generated from an online Digital Elevation Model (with 1” resolution), and a snow/no-snow pixel-level classifier (with 90% accuracy).
- An algorithm that transforms mountain camera position, peak metadata, and snow masks into data series of virtual snow indexes for a mountain viewpoint, previously introduced in [8, 9]. Such indexes, albeit not directly comparable to available ground measures, exhibit a strong correlation with meteorological data series.
- A multi-objective water management model and simulation framework for the design and evaluation of optimal operating policies conditioned on multiple variables such as the day of the year, the lake level, the SWE, the virtual snow indexes, and more, which can be used to assess the operational value of virtual snow indexes.
- As byproducts of the content processing pipeline, we have produced a very large public data set of Alpine mountain images and a gamified web portal, where users can cooperatively access and enrich content¹.

2. RELATED WORK

Web media mining for environment studies A growing body of research studies the potential of low cost, user generated content in environmental applications, with different content types, including text, images, videos, GPS tags, and cellular phone traces. Zhang et al. [25] predict snow and vegetation cover using geo-tagged Flickr photos. The analysis is based on the tags associated with the photos and on the image visual features. Daume et al. [4] approach forest monitoring with social media data (tweets), analyzed to extract various ecosystem information types, trends, predictions and alerts. Social media are also exploited for disaster management: De Longueville et al. [5] report a study of fire propagation monitored through tweet distributions. None of these approaches evaluates the contribution of web content to the performance of environmental models. In [18], the

¹<http://snowwatch.polimi.it>

authors manually monitor YouTube videos to derive a water level time series for a Saudi Arabian cave, which helped locate the water source. In our work, media monitoring and information extraction are completely automated.

Mountain image analysis. Traditionally, snow is monitored through manual measurement campaigns, permanent measurement stations, satellite photography, and, recently, also with terrestrial photography. Although several approaches monitor snow processes by means of short-range visual content analysis, all approaches (e.g., [20, 19]) rely on cameras designed and positioned ad hoc by researchers, and are not applicable to user-generated web content created in uncontrolled conditions. Other work addressed mountain peak identification in public photos (a key problem to retrieve snow information from public images) [1] and the segmentation of the image region corresponding to a certain mountain in snow covered areas [20, 19]. All these approaches do not provide an environmental evaluation of the utility of the data extracted with the proposed techniques. In this paper, we evaluate the utility of virtual snow indexes computed from web content collected with such pipelines, on a case study of water availability prediction and multi-objective allocation.

Water management with hydrologic information. The availability of data at increasingly higher temporal and spatial resolution creates an opportunity to enhance real-time understanding of water systems and to improve prediction of their future evolution, ultimately increasing quality of the decisions. Yet, many large water projects worldwide had their operations designed in prior decades, with rules based on very simple data, such as current inflow and previous release volumes [16]. Numerous studies have attempted to improve water reservoirs operations by using information selected on the basis of operators’ experience, such as observations of the previous period’s inflows [22], simplified models of hydrologic variables [6], or streamflow forecasts [21]. As for the latter, the use of reliable inflow forecasts is beneficial in most situations. Yet, its real value is often problem-specific and depends on the system’s dominant dynamics and the objectives considered [24]. For example, using short-term inflow forecasts generally improves reservoir operations for flood control; for other objectives, such as water supply, medium and long term streamflow forecasts are required.

3. OVERVIEW OF THE APPROACH

The goal of this work is to experimentally assess the operational value of information derived from public web media content, specifically from mountain images contributed by users and existing webcams, to support environmental decision making in a snow dominated context. An automatic system crawls geo-located images from heterogeneous sources at scale, checks the presence of mountains in each photo, identifies individual peaks, and extracts a snow mask from the portion of the image denoting a mountain. The assessment requires a water management problem where snow information is a determinant input to the system operation and performance can be quantified. We use a water management model for Lake Como, and evaluate the impact of snow-related data extracted from web content as additional input to the lake operating policy.

The study site. Lake Como is a regulated lake in Northern Italy with an active storage capacity of 254 Mm³ and fed by a 3,500 km² catchment. The hydro-meteorological

regime is the typical Alpine one, with scarce discharge in winter and summer, and peaks in late spring and autumn due to snowmelt and rainfall, respectively. Snowmelt from May to July is the most important contribution to seasonal lake storage, but the operations of a number of hydropower reservoirs in the upstream lake catchment alter the natural hydrologic regime. The water stored in the lake can be used in different ways according to two main competing objectives. Farmers downstream would like to save it for the summer, when the natural inflow is not sufficient for irrigation. Yet, storing water increases the lake level and, consequently, the flood risks, which would be instead minimized by keeping the lake level low. The ability to predict future water availability, particularly from snow melt, is key for an optimal water management strategy. The competing interests of flooding and irrigation can be modeled using the following quantitative objectives:

Flooding: the average annual number of flooding days, defined as days when the lake level h_t is higher than the flooding threshold ($\bar{h}=1.24$ m), i.e.,

$$J^{flood} = \frac{1}{N_y} \sum_{t=1}^{t_{fin}} \Lambda(h_t) \quad \text{where } \Lambda(h_t) = \begin{cases} 1 & \text{if } h_t > \bar{h} \\ 0 & \text{otherwise} \end{cases}$$

Irrigation: the daily average squared water deficit w.r.t. the daily downstream demand w_t , subject to the minimum flow constraint q_t^{MEF} to ensure adequate environmental conditions in the Adda River, i.e.,

$$J^{irr} = \frac{1}{t_{fin}} \sum_{t=1}^{t_{fin}} \max(w_t - \max(r_{t+1} - q_t^{MEF}, 0), 0)^2$$

where r_{t+1} is the water volume released in the time interval $[t, t + 1)$. The release r_{t+1} coincides with the release decision u_t unless a correction is needed in order to take into account the legal and physical constraints on the reservoir level and release. The quadratic formulation aims to penalize severe deficits in a single time period, while tolerating more frequent, small shortages.

4. WEB CONTENT PROCESSING

Two image sources are used: we crawl $\sim 2k$ touristic webcams in the Alpine area and search Flickr for geo-tagged user-generated mountain photos in a $300 \times 160km$ Alpine region. Both image types carry information about the location where the image is taken, but require estimating the orientation of the camera during the shot, identifying the visible mountain peaks, and filtering out images not suitable for snow analysis (e.g., due to fog, rain etc.). The two multimedia processing pipelines, shown in Figure 2, share common steps but also have differences: webcams produce a temporal series of images of the same view, so that *only one webcam image* needs to go through the relevance classification and peak identification steps, whose results apply to the entire time series. Instead, *all crawled user-generated photos* need pre-filtering, for discarding irrelevant content before processing them for orientation and peak detection.

4.1 Webcam processing

The registered webcams capture images every 1 to 60 minutes, thus ensuring temporal density incomparably higher than any remote sensed data. On the other hand, their spatial density is lower than that of user-generated photos, be-

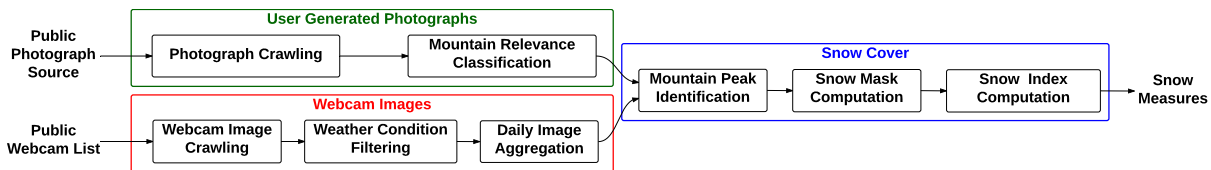


Figure 2: Schema of the web media content processing pipelines.

cause they concentrate near popular touristic destinations. We identified more than 3500 candidate webcams in the Alpine area from touristic, meteorological, and skiing webcam directories, and manually filtered them, removing those that were not framing significant mountain slopes, retaining nearly 2k webcams. A web crawler checks each webcam at 1' frequency and processes all new images. In this way, we obtain, for each camera, from 10 to 1.5k images per day, depending on update frequency and working hours. Due to bad weather conditions, not all images can be exploited for estimating snow cover. A manual screening of 1000 images crawled from 4 webcams revealed that 67% were not suitable for snow analysis. To retain only processable images, a *weather conditions filter* automatically discards images acquired during bad weather conditions, which are identified by checking for occlusions of the mountain skyline, as follows: *For each webcam*, we manually annotate its skyline, and a binary skyline neighborhood mask L identifies all the pixels which are distant less than a certain value (in our case empirically set to 4% of the image height) from at least one skyline point. Then, *for each webcam image*, we apply standard edge detection and compute its binary edge map E , which identifies pixels belonging to the skyline. To check for occlusions, a skyline visibility score is defined as $v = f(E \cdot L) / f(L)$, where \cdot denotes the pixel-wise product between two images of the same size and $f(\cdot)$ is a function that, given an image, returns the number of columns that contain at least one non-zero entry. The value of v is in the interval $[0, 1]$ and can be intuitively interpreted as the fraction of the skyline that is visible in a given image. We retain only those images for which $v \geq \bar{v}$, where \bar{v} is a threshold (empirically set to 0.75). The filtering method retains images with good skyline visibility, although clouds might still be present and interfere with the estimation of the snow cover. The effect of such transient clouds is mitigated by the next webcam image processing step.

Daily image aggregation. Good weather images might suffer from challenging light conditions (solar glares and shadows) and moving obstacles (clouds and persons in front of the webcam). At the same time, snow cover changes slowly over time, so that one (good) measurement per day is sufficient. Therefore, it is possible to aggregate all images collected in a day, to obtain a single daily image, which is both robust to transient occlusions and sufficiently representative for analysis. A simple median aggregation proved able to effectively remove transient occlusions and glares. Given a daily sample of N images I_1, \dots, I_N , the Daily Median Image (DMI) is defined as

$$DMI(x, y) = \text{med}\{I_1(x, y), I_2(x, y), \dots, I_N(x, y)\},$$

where $\text{med}\{\cdot\}$ is the median operator applied to the image pixel values. Figure 3 shows a DMI obtained from 11 daily images, which attenuates transient illuminations and removes the persons standing in front of the webcam.



Figure 3: An example of a Daily Median Image (right) performed on 11 daily images (left).

A challenge in the creation of DMIs lies in strong winds, which may produce a blurry aggregated image. To overcome this issue, image registration is performed w.r.t. a reference frame (the first image of the day). A global offset is computed by means of the cross-correlation between the two skyline edge maps and each image is compensated by this offset before computing the DMI.

Identifying mountain peaks. A DMI per webcam is processed to identify peaks, with a procedure based on the alignment between the image and a virtual terrain model². Given a photo and the metadata extracted from the EXIF container (geo-tag, focal length, camera model and manufacturer), it is possible to perform a matching with a 360° panoramic view of the terrain synthesized from a Digital Elevation Model (DEM). The method proceeds in steps: *Preprocessing* - estimation of the horizontal Field Of View (FOV), edge extraction, noise edge filtering; *Global alignment* - estimation of the best overlap between the photograph and the panoramic view through Vector Cross Correlation (VCC) applied to the respective edge maps; *Local Alignment* - improving the precision of the position of each peak with a separate VCC procedure. If a webcam image does not contain EXIF data, its FOV cannot be estimated, and the alignment cannot be performed. In this case, the image is posted to an ad-hoc developed crowdsourcing web platform, where volunteers can help find the correct FOV and alignment manually. This step does not induce a significant overhead, because it is executed only once per webcam.

4.2 User generated photograph processing

Webcams are relevant data sources, with high temporal resolution but invariable positioning. Tourists are another valuable source of images, with a potentially more uniform spatial distribution. Also, if properly activated, crowds can engage in specific campaigns and act as a collective webcam that could be pointed virtually to the desired target. Differently from webcams, user generated photos are mined from sharing sites by geo-search, whose results may contain completely irrelevant images. Search outputs must be filtered, to retain only mountain pictures. Analogously to webcam images, once a photograph is classified as relevant, it must be subjected to peak labeling, to identify the mountain view it portrays and extract snow information. Flickr

²The procedure is the same applied to crowdsourced images.

was selected, because it contains a large number of public images, many with the geo-tag in their EXIF container. A continuous search system was built, which queries images within a 300×160 km region in the Alps; as of now, the Flickr search pipeline has examined $\sim 600k$ candidate photos. To train the relevance classifier, we collected ground truth labels: 6940 randomly selected photos taken above an altitude of 500 meters were processed in a crowdsourcing experiment, in which workers had to label images based on the presence of a mountain skyline. The aggregated label was obtained by majority voting. Approximately 23% of the images were classified as positive. Then, the automatic mountain classifier was built as follows. From each training image a fixed-length feature vector representing its visual content was constructed. To create a balanced dataset, we retained all the positive samples and randomly selected the same number of negative samples. Then, we used $\sim 70\%$ of the samples for training and validation and $\sim 30\%$ for testing. The encoded feature vectors were fed to a SVM classifier using a χ^2 kernel. To learn the optimal values of the C and γ kernel parameters of the SVM classifier, we adopted k -fold cross validation, with $k = 5$ for the grid search. The mountain photos classified as relevant are then subjected to the same mountain peak identification procedure as webcam images.

4.3 Experimental evaluation

The content processing pipeline has been evaluated experimentally. This required us to assess 3 components: the weather condition filter (used for webcams), the mountain relevance classifier (used for UGC) and the peak alignment algorithm (used for both webcams and UGC).

Weather condition filter. We manually labeled 1000 images collected from 4 webcams, with the tag “good weather”, if the mountain area was completely visible, or “bad weather” otherwise. Due to the high temporal frequency of webcam image acquisition, many images are available; thus, the threshold parameter \bar{v} was set to a value ensuring low FPR (0.75), obtaining a TPR equal to **87.4%** at FPR **3.5%**.

Mountain relevance classifier. Evaluation compared 8 configurations, by pairing 4 local and global image feature descriptors (Dense SIFT, HOG2x2, SSIM and GIST) and 2 vector encodings: Bag-of-Visual-Word (BoVW) and Fisher vector encoding. The best configuration proved to be: Dense SIFT, BoVW encoding, SVM with parameters values $C = 3.3$, $\gamma = 0.66$; this configuration obtained **95.1%** accuracy, **94.0%** precision, and **96.3%** recall on the test set.

Peak identification. We manually inspected 200 photographs and the virtual panoramas generated from the EXIF metadata and DEM, to make sure that a plausible match existed (e.g. a match could be impossible due to bad GPS tag), obtaining 162 good photos. Ground truth peak alignment data were generated by an ad-hoc developed alignment tool, which allows users to define the correct orientation of the image and fix the position for each peak mentioned in the virtual panorama. Considering a tolerance of 3deg, **75%** of the image orientations were correctly estimated; this percentage grows to **77.6%** and **81.6%** in absence of clouds and nearby mountain slopes, respectively. The average positioning error of peaks resulted to be **0.78** deg.

Execution times. The automatic alignment procedure dominates the entire image processing time. The generation of $1500px \times 12000px$ panoramic view requires approximately

1s with a GeForce GTX 850M graphic card. The alignment of an image to the virtual panorama requires approximately 30s on an OpenStack virtual instance with 4 $2.5GHz$ VCPUs and 8Gb of RAM.

4.4 Snow index computation

Once an image is classified as relevant and its peak identified, snow information can be extracted and associated with the mountain(s) that appear in it, at the time the image was taken (or at the day, in case of a DMI). A *virtual snow index* is defined as a real value representing the snow information extracted from the photo or from the DMI. When used as input to environmental models, these indexes do not necessarily need a physical interpretation (e.g., like snow depth), as long as they reflect the dynamics of snow distribution. The snow indexes used in the case study are determined as follows. Let I denote an image and M a binary mask having the same size as I , where $M(x, y) = 1$ indicates that the pixel $I(x, y)$ of the image belongs to the mountain area, or $M(x, y) = 0$ otherwise. A *snow mask* is defined as the output of a pixel-level binary classifier that, given I and M as input, produces a mask S that assigns each pixel a binary label denoting the presence of snow. We computed snow masks using the Random Forest supervised learning classifier with spatio-temporal median smoothing of the output. The classifier achieves 90.0% precision at 91.1% recall, outperforming existing methods for pixel level snow detection. From the snow mask S , the snow indexes are computed as follows. Let H denote a real value map having the same size as I , where $H(x, y)$ denotes the altitude of the terrain in the point that corresponds to $I(x, y)$ (e.g., altitude in meters, that can be estimated from the projection of the pixel the on DEM), for each (x, y) such that $M(x, y) = 1$ (i.e., for pixels representing points within the mountain region of the image). M and H can be obtained during the mountain peak identification phase, because each pixel of the photo gets aligned with a pixel of the virtual panorama; the latter carries information not only about the edges of the mountains, but also about the type (terrain/sky) and altitude of each DEM pixel. Let \hat{H} denote the linearly normalized version of H , where the minimum (maximum) altitude corresponds to 0 (1). Then, a *virtual snow index* for an image I is defined as $\sum_{(x,y)|S(x,y)=1} vsi(x, y)$, where vsi is a virtual snow index function that transforms a pixel position into a snow relevance coefficient. We tested three different snow feature functions:

$$vsi^1(x, y) = \hat{H}(x, y)^2, vsi^2(x, y) = \frac{\hat{H}(x, y)}{N_{x,y}}, vsi^3(x, y) = 1$$

where N is the number of horizontal bands in which we split the mountain area of the image and $N_{x,y}$ denotes the number of mountain pixels belonging to the same band of a pixel $I(x, y)$. The first snow index weights each snow-covered pixel quadratically w.r.t. its altitude, the second one weights each snow-covered pixel linearly w.r.t. its altitude and normalizes the score w.r.t. the number of pixels contained in the same band, and the third one weights each snow-covered pixel uniformly regardless of its altitude. The values for the three indexes are computed for each day and their operational value is assessed in Section 6.

4.5 Content selection for the case study

The dataset contains more than 2.5M mountains images

located across the Lake Como catchment; such images are produced by 62 webcams and include also more than 100k photos produced by users. However, not all relevant images are directly exploitable for the assessment; environmental models require a very long observation period: a statistically significant evaluation *requires observations spanning multiple years*, to cope with seasonal effects. We started collecting images in Dec. 2014, and therefore most sources lack a long enough time series to be usable as input. A manual search found historical images of a few webcams and aggregated them to the dataset. Specifically, we found one webcam with enough historical data, which was chosen for the experiments. The webcam is placed in Livigno and the observation period comprises 818 days, from Jan 1, 2013 to Mar 29, 2015. The mountain framed by the webcam is positioned inside the Como lake catchment and its snow level is known to affect the lake water dynamics. Even with a single webcam, the experimental results described in Section 6 demonstrate a significant utility of the snow-related data. We plan to carry out experiments at larger scale in the lake catchments of the entire Alpine arc, as the dataset will grow thanks to continued crawling and the crowdsourcing campaigns performed with the mobile photo collection application described in Section 8.

5. WATER MANAGEMENT OPTIMIZATION

The assessment of the operational value of snow information is done by comparing the performance of alternative operating policies for the regulation of Lake Como. A *policy* is a function returning the quantity of water to be released u_t at each time instant $t = [0 \dots T - 1]$, as dependent upon an information vector \mathbf{z}_t , i.e., $u_t = p(\mathbf{z}_t)$. Based on the input information, different policies are employed: 1) A *perfect* control policy, an ideal policy used as an upper bound of the system performance, which makes always the optimal decision based on perfect knowledge of current and future system conditions. 2) A *baseline* control policy, which considers only limited information (day of the year and current lake level). 3) An *informed* control policy, which exploits additional information, including snow-related data. Specifically, two informed policies are contrasted, one exploiting official snow data from ARPA (*official data policy*) and one using the virtual snow indexes computed from web content (*web data policy*). The assessment quantifies how closer the informed control policies get to the perfect one, in comparison to the baseline.

This evaluation methodology, called Information Selection and Assessment (ISA) framework [14], consists of 3 steps: (i) Quantification of the expected value of perfect information, i.e., the potential for improving operations under the assumption of perfect knowledge of future conditions; (ii) Automatic selection of the most valuable information to improve current operations; (iii) Evaluation of the selected information on the resulting control policy performance.

5.1 Expected Value of Perfect Information

The Expected Value of Perfect Information (EVPI) is the performance gain that can be achieved under the assumption of perfect foresight on the future [23]. If the value of EVPI is small, a limited information policy already performs close to the best strategy and thus the benefit of additional input data approximating future system conditions is limited. The availability of perfect knowledge of the future exter-

nal drivers (e.g., lake inflows) is equivalent to assume that the operator is an omniscient oracle implementing a Perfect Control Policy (PCP), consisting of an optimal sequence of release decisions $u_{[0, T-1]}^{PCP}$, conditioned on the current system status (i.e., the time instant t and the current lake level l_t), and on the perfect knowledge of the future inflows. In the experiments illustrated in Section 6, the PCP is built by solving the control policy design problem over a 2-year horizon in which the sequence of inflows is known. This is a standard nonlinear optimization problem and can be solved by either a local optimization method (e.g., gradient-based) or a global optimization method (e.g., direct search). Alternatively, since the objective functions in our application are time-separable, we use deterministic dynamic programming (DDP), which is more efficient and provides an almost exact solution.

PCP performance (\mathbf{J}^{PCP}) has a relative value, because it depends on the physical characteristics of the system, e.g., the ratio between the lake capacity and its inflow. The EVPI has hence to be estimated as the distance between \mathbf{J}^{PCP} and the performance of a Baseline Control Policy (BCP), defined as a simple closed-loop control policy, where \mathbf{z}_t includes the time index t and the current lake level l_t .

In a single-objective scenario, the EVPI is simply the difference between the (scalar) performance of the PCP and BCP. In a multi-objective case, the evaluation is more complex; the performance objectives \mathbf{J}^{PCP} and \mathbf{J}^{BCP} are vector functions and the solution is not unique, but rather a set of Pareto optimal solutions (Pareto Front). Among the commonly used metrics (see [17]), the ISA framework adopts the hypervolume indicator (*HV*), which captures both the proximity of the Pareto Front \mathbf{J}^{BCP} to the ideal one \mathbf{J}^{PCP} as well as the distribution of the BCP solutions in the objective space. The hypervolume measures the volume of objective space dominated (\preceq) by the considered set of solutions (S). Then, the *HV* indicator is defined as the ratio of the hypervolumes of the solutions produced by BCP and PCP:

$$HV(BCP, PCP) = \frac{\int \alpha(\mathbf{s}_{BCP}) d\mathbf{s}_{BCP}}{\int \alpha(\mathbf{s}_{PCP}) d\mathbf{s}_{PCP}}$$

$$\alpha(\mathbf{s}) = \begin{cases} 1 & \text{if } \exists s' \in S \text{ such that } s' \preceq \mathbf{s} \\ 0 & \text{otherwise} \end{cases}$$

If policy A has a value of HV greater than a policy B, the solutions produced by A dominate a larger fraction of the objective space, which means that A is better than B in pursuing the multiple objectives of the system. The EVPI can then be computed as the difference between the *HV* of PCP (i.e., 1 by definition) and the *HV* of BCP.

5.2 Most Valuable Information Selection

A large value of EVPI indicates that a control policy endowed with more information can approach the performance of the ideal, omniscient one. The ISA methodology helps identify the input information that enables the informed policy to approximate as much as possible the optimal sequence of decisions $u_{[0, T-1]}^{PCP}$. The set Ξ_t of candidate inputs may comprise *exogenous variables*, i.e., variables that are observed in the time interval $[0, T - 1]$ but are not part of the problem formulation; examples are rainfall, temperature, snow presence, etc. Since Ξ_t can comprise redundant and collinear variables, its smallest subset $\mathbf{I}_t \in \Xi_t$ that carries the most valuable information must be identified, as the

Algorithm 1 Iterative Input Selection

Inputs: a dataset \mathcal{F} of candidate inputs \mathbf{v}^i and the output variable to explain v^o .
Initialization:
Set $\mathcal{V} \leftarrow \emptyset$, $\hat{v}^o \leftarrow v^o$, $D_{old} \leftarrow 0$
Iterations: repeat until stopping conditions are met
- select the most relevant input $v^* \in \mathbf{v}^i$ to explain \hat{v}^o
- **if** $v^* \in \mathcal{V}$, **return** \mathcal{V} **endif**
- $\mathcal{V} \leftarrow \mathcal{V} \cup v^*$
- $\hat{m}(\cdot) \leftarrow \text{Extra-Trees}(\mathcal{F}, v^o, \mathcal{V})$
- $\hat{v}^o \leftarrow v^o - \hat{m}(\cdot)$
- $\Delta D \leftarrow D(v^o, \hat{m}(\cdot)) - D_{old}$
- $D_{old} \leftarrow D(v^o, \hat{m}(\cdot))$
- **until** $\Delta D < \varepsilon_D$
return \mathcal{V}

one that best explains the optimal sequence of decisions. Several techniques can be used to solve this feature selection problem [11], such as cross-correlation analysis, mutual information analysis, or input variable selection methods. We use the hybrid model-based/model-free Iterative Input Selection (IIS) algorithm (Algorithm 1), which can approximate strongly non-linear functions and scale to large datasets made of long time series and many candidate variables [11]. Given a generic output variable v^o and the set of candidate inputs \mathbf{v}^i , IIS first ranks the inputs w.r.t. a statistical measure of significance and adds the best performing input v^* to the current set of selected variables \mathcal{V} . This step avoids the inclusion of redundant variables: after an input is selected, all the other inputs highly correlated with it will rank low in the next iterations. Then, the algorithm estimates a model of v^o with input \mathcal{V} , such that $v^o = \hat{m}(\mathcal{V})$, and estimates the model performance with a distance metric D (e.g., the coefficient of determination) as well as the model residuals ($v^o - \hat{m}(\mathcal{V})$), which become the new output at the next iteration. The algorithm stops when the next best input variable selected is already in the set \mathcal{V} , or when over-fitting conditions are reached. Among the many alternative model classes, IIS relies on extremely randomized trees (Extra-Trees), a tree-based method proposed by [12] that was empirically demonstrated to outperform other models in terms of modeling flexibility, efficiency, and scalability with respect to the input dimensionality. Moreover, Extra-Trees structures can be exploited to infer the relative importance of variables, as required for their ranking [3].

5.3 Expected Value of Sample Information

After selecting the most valuable information $\mathbf{I}_t \subset \Xi_t$, the next step is to design the Informed Control Policy (ICP) that exploits such information to make decisions. The ICP is defined by extending the input \mathbf{z}_t of the baseline control policy with the selected information, i.e., $\mathbf{z}_t = (t, l_t, \mathbf{I}_t)$, and searching the optimal control policy with approximate dynamic programming methods. We use the evolutionary multi-objective direct policy search (EMODPS), a simulation-based technique that combines direct policy search, nonlinear approximating networks, and multi-objective evolutionary algorithms [13]. EMODPS exploits the parameterization of the control policies p_θ and explores the parameter space Θ to find a policy (p_θ^*) that optimizes the expected system performance (J_θ , conventionally assumed to be a cost), i.e., $p_\theta^* = \arg \min_{p_\theta} J_\theta$ where the policy p_θ is parameterized by

Algorithm 2 Evolutionary Multi-Objective Direct Policy Search.

Initialization:

Generate a random parameter values population $\{\theta^1, \dots, \theta^P\}$

Iterations: repeat until stopping conditions are met

- generate a trajectory τ^i via model simulation according to the stochastic transition function $\mathbf{x}_{t+1} = f(\mathbf{x}_t, \mathbf{u}_t, \varepsilon_{t+1})$ and following the policy p_{θ^i} (with $i = 1, \dots, P$)

- compute performance $J_{\theta^1}^i, \dots, J_{\theta^P}^i$, with $i = 1, \dots, P$

- generate new population by selection, crossover and mutation w.r.t. the best individuals (i.e., non Pareto-dominated solutions)

parameters $\theta \in \Theta$ and the problem is constrained by the dynamics of the system. Finding p_θ^* is equivalent to finding the corresponding optimal policy parameters θ^* . A tabular version of the EMODPS method is illustrated in Algorithm 2.

In general, we expect the ICP to fill the performance gap between the upper and lower bound solutions (i.e., the PCP and BCP), and to produce a performance \mathbf{J}^{ICP} as close as possible to \mathbf{J}^{PCP} . The benefit associated to the use of the selected information is called *Expected Value of Sample Information* (EVSI) and can be quantified by means of the same metrics used for the evaluating the EVPI (see Section 5.1).

6. EXPERIMENTS AND RESULTS

The experimental setting is characterized as follows.

Perfect Control Policies: PCPs are designed via Deterministic Dynamic Programming over 2 years of historical data (2013-2014). The weighting method is used to convert the 2-objective problem (flooding and irrigation) into a single objective, via convex combination. The PCPs are designed under the assumption of perfect foresight on the future at the moment when decisions are taken, i.e., we assume perfect knowledge on the lake inflows over the evaluation period.

Baseline Control Policies: BCPs are defined as traditional control policies conditioned on the day of the year t and on the lake level l_t . These policies are designed via EMODPS. *Candidate exogenous variables and automatic selection of information:* to build the informed control policies ICP, we evaluate the contribution of adding exogenous variables from the official monitoring network: previous day spatial precipitation in the Lake Como catchment (P_t), previous day freezing level (FL_t), upstream hydropower storage (sHP_t), previous day release from hydro-power reservoirs (rHP_t), and weekly estimate of snow water equivalent (SWE_t), elaborated by ARPA from ground stations and MODIS data. In addition to official variables, we consider the three virtual snow indexes computed from web images. The most valuable information is identified with the IIS algorithm.

Informed Control Policies: ICPs are designed via EMODPS, with the control policies parameterized as Gaussian Radial Basis Functions, which have been proved effective in multi-objective control problems with exogenous input [13, 14]. For the optimization, the self-adaptive Borg Multi-Objective Evolutionary Algorithm [15] is used, which is robust and efficient across diverse multi-objective problems. Each optimization is run for 2 million function evaluations, with the simulation step performed over the same 2-years horizon. To improve solution diversity and avoid dependence on randomness, the solution set from each formulation is the result

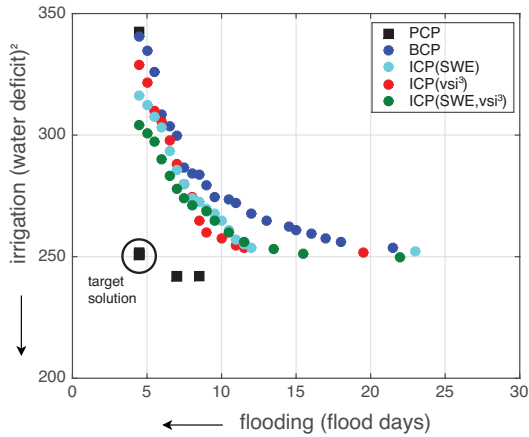


Figure 4: Performance of PCP (black squares), BCP (blue circles), and alternative ICPs with different information (SWE in cyan, vsi^3 in red, SWE and vsi^3 in green).

of 30 random trials. The final set of Pareto optimal policies for each experiment is defined as the set of non-dominated solutions from the results of all the optimization trials.

6.1 Quantifying the EVPI

The first step of the ISA framework (Section 5) estimates the Expected Value of Perfect Information by contrasting PCPs and BCPs. Figure 4 shows the performance of the PCPs (represented by black squares) evaluated over the horizon 2013-2014. The blue circles represent the performance of the BCPs (traditional control policies conditioned on the day of the year and the lake level). The performance of the ICPs (red, cyan, and green circles) is discussed later on in Section 6.3. The arrows on the axes point in the direction of increasing preference, with the best solution located in the bottom-left corner of the figure. Visual comparison of the Pareto Fronts shows that the potential for improvement over BCPs is large: the gap between basic information and the perfect knowledge is substantial in terms of both operating objectives, as represented by the area between the black squares and the blue points. A first qualitative analysis can be done focusing on a specific target PCP solution (circled in the figure), which represents a potentially good compromise between flood control and irrigation supply. However, it seems to be difficult to turn this solution into an actual regulation of the lake with BCP: while the extreme solutions in the PCP and BCP fronts, representing the independent optima for flooding and irrigation, are almost equivalent, the maximum distance between the two fronts is in correspondence with the selected target solution. This motivates searching for ICPs that can fill the gap. Quantitative EVPI assessment is provided by the HV indicator in Table 2, where the difference between BCP and PCP is equal to 0.29, confirming the gap between Perfect and Baseline Control Policies.

6.2 Exogenous Variables Selection

The question whether snow information can help making more informed decisions is addressed by using the ISA framework to identify the most informative exogenous variables $\mathbf{I}_t \subset \Xi_t$. We first evaluate the day of the year and the

lake level together will all the exogenous variables except our virtual snow indexes, to check if the official snow information is relevant. The rationale for retaining the day of the year and the lake level is to extend the BCP and avoid selecting exogenous variables correlated with t or l_t . Then, we contrast official snow information with virtual snow indexes in Section 6.3 and 6.4. We perform 20 runs of the IIS algorithm to filter the randomness associated to the construction of the Extra-Trees models. Despite the limited length of the time series (only 2 years), which introduces some variability across the runs, the best result consistently selects as most valuable information the day of the year (t), the lake level (l_t), and the official ARPA estimates (SWE_t). This confirms the key role of snow dynamics in the Lake Como system. Using the 3 variables selected, the Extra-Trees model approximates the optimal sequence of release decisions $u_{[0,T-1]}^{PCP}$ attaining a model performance, evaluated using the coefficient of determination (D), equal to 0.639. Table 1 shows the contributions of variables and statistics over the 20 repetitions.

Table 1: Variables selected by the IIS algorithm.

Variable	Best-run	Selection frequency, 20 runs	Average contribution (R2), 20 runs
t	0.231	100%	0.334
l_t	0.348	85%	0.194
SWE_t	0.060	45%	0.108

6.3 Benefits of official snow information

To quantify the value of the official ARPA snow water equivalent, we assess the performance of the ICPs conditioned on the information vector $\mathbf{z}_t = (t, l_t, SWE_t)$. The resulting policies $ICP(SWE)$ are represented by cyan points in Figure 4. The comparison of the performance of BCP and $ICP(SWE)$ shows a relevant contribution of the official snow information: this is due to an improved medium-long term foresight, as snow information provides useful insight about the expected water availability during the next summer, when the irrigation demand is high and the conflict between flooding and irrigation is critical. A quantitative evaluation of the EVSI associated to this variable is given by HV reported in Table 2: HV increases from 0.7079 to 0.7848 (i.e., +10.9%) when moving from BCP to $ICP(SWE)$.

6.4 Benefits of web snow information

The question of whether the virtual snow indexes (vsi^k) defined in Section 4.4 can complement the official ARPA SWE data is addressed through the following experiments: first, we replace the ARPA SWE variable with each virtual snow index vsi^k and analyze the performance of the corresponding policies $ICPs(vsi^k)$. Second, we explore the possibility of complementing, instead of replacing, the ARPA SWE variable with the virtual snow indexes, by evaluating the performance of ICPs conditioned on the information vector $\mathbf{z}_t = (t, l_t, SWE_t, vsi_t^k)$. We report only the results obtained using the third snow index vsi^3 , because it consistently outperforms the other two indexes. The comparison of $ICP(SWE)$ and $ICP(vsi^3)$, represented by red points in Figure 4, shows that the value of the virtual snow index is comparable to, and sometimes higher than, the

one of the ARPA SWE. In fact, the red Pareto Front intersects the cyan one, with some red solutions outperforming the cyan ones in the compromise region of the front, close to the target PCP. This observation is confirmed by the corresponding values of HV , with $ICP(vsi^3)$ attaining a higher value than $ICP(SWE)$, which corresponds to a 11.6% improvement with respect to the BCPs. Finally, the performance of the ICPs conditioned on both SWE_t and vsi^3 (green points in Figure 4) outperforms both BCPs and ICPs(SWE). Such superiority is certified by the values of HV : $ICPs(SWE, vsi^3)$ attains a value equal to 0.816, which corresponds to a 15.2% improvement with respect to the BCPs and a 4% improvement with respect to $ICPs(SWE)$. These results suggest a significant potential for complementing the official ARPA SWE estimate with virtual snow indexes derived from public web media.

Table 2: Quantification of Expected Value of Perfect and Sample Information in terms of hypervolume indicator.

Policy	HV	ΔHV
BCP	0.7079	-
$ICP(SWE)$	0.7848	+10.9%
$ICP(vsi^3)$	0.7898	+11.6%
$ICP(SWE, vsi^3)$	0.816	+15.2%
PCP	1.0	-

7. DISCUSSION

In this paper we have presented the results of an integration effort of multimedia and environment research, proving that low-quality, low-cost, yet widely available, public content can provide input that improves the performance of a practical environmental model in a quantifiable manner. The proposed approach exemplifies the opportunities, but also the challenges, of applying multimedia processing techniques to real-world environmental problems.

Opportunities Multimedia research has attained robust methods and high accuracy in many knowledge extraction tasks that could radically change the way in which environment monitoring is performed. The interplay of three factors makes the integration of multimedia and environment research particularly relevant and timely: 1) the increase of user generated content, which is now turning also to real-time video; 2) the deployment of IoT infrastructures and low-cost cameras, which makes ground sensing affordable for novel applications, including e.g., environment and agriculture monitoring; 3) the impact of climate change, which is increasing the frequency and severity of extreme events, putting traditional monitoring networks under stress.

Open Challenges Traditional environment research generally relies on complex models, which encode the properties of the investigated system and thus require input data endowed with a precise physical interpretation, often collected with manual procedures and dedicated equipment. On the other hand, the information that can be extracted, automatically, accurately, and at scale, from public content is much more noisy and simpler in format and meaning than that employed by many state-of-practice models. The fundamental challenge is to identify the “overlap region” where the knowledge extracted with multimedia processing methods can improve the performance of practical environmental models.

The problem addressed in this paper is an almost ideal one, where several factors concur to make the case tractable: public mountain images are abundant and with sufficient spatio-temporal coverage, can be processed (offline) with high accuracy, and contain a signal (snow presence) that, albeit simpler than the parameters used by snow process models based on physical laws, is relevant for a specific environmental problem. However, future research can generalize the proposed framework to more challenging scenarios, along a number of directions, including: the type of input data (e.g., video), the processing requirements (e.g., online and real-time), the spatio-temporal dynamics, and the environmental problem addressed. For example, river basin occlusion is a relevant problem for hydrogeological risk prevention, because excessive sediment and vegetation can cause overflow: multimedia research could exploit (already existing) webcams deployed for human-assisted river bed surveillance, possibly complemented by user generated, crowdsourced images, and help estimate the river flow, which is connected to the risk of flooding during heavy rainfall. This scenario generalizes the research agenda towards another type of image processing and the analysis of the spatio-temporal dynamics of a different environment phenomenon. An even more challenging case of fast-dynamics, real-time scenario is exploiting real-time user generated video content for addressing event-based environmental monitoring. For example, flood level and water speed information extracted from user-generated video could be used in input to flood propagation prediction models based on DEM data, to forecast the reach and impact of flood, so to alert citizens and adjust evacuation plans. This scenario generalizes the research agenda towards more complex input, quasi-realtime constraints, and the analysis of the fast spatio-temporal dynamics of an environment phenomenon. Furthermore, multimedia analysis for environmental data should move from “extract already available environmental data from new media sources” paradigm to “extract novel environmental data and prove that it is complementary to existing one”. We believe that this impact-focused approach will decrease the reluctance of the environmental science community to adopt novel multimedia analysis techniques.

8. CONCLUSIONS AND FUTURE WORK

In this paper we tested the hypothesis that public web content, either crowdsourced or gathered from ground sensors, can be effectively used in input to environmental decision models. The experiments, although conditioned by the limited duration of the time series available, show that it is possible to use virtual snow indexes computed from mountain images to design more informed, and thus improved, water management strategies. Preliminary results show that even a single webcam stream is capable of providing valuable information to the management policy of Lake Como and improves the system performance w.r.t. the conflicting objectives of irrigation water supply and flood risk minimization. Using simulation, we demonstrated that the virtual snow indexes obtained from public web media content can replace official snow measurements derived from permanent ground stations and satellite imagery without performance loss; also, they can complement official snow information yielding further performance improvement, which shows that the two data sources are not redundant. As time passes and we acquire longer time series for more

relevant mountains and more user generated photos, the performance of the policies conditioned on web content inputs is expected to increase. In parallel, we are building an augmented reality mobile app for mountain photo sharing. The app overlays in real time peak names over photo and videos, with high accuracy. The user can save her photos, with the mountain landscape nicely adorned with peak names, in our mountain photo portal, correct the automatic alignment, and share the result on popular social networks, inviting more people to do the same. As a last objective, we are porting the architecture to different environmental problems where the same approach applies: sediment monitoring in river beds and vegetation monitoring in mountain regions.

9. REFERENCES

- [1] L. Baboud, M. Cadik, E. Eisemann, and H.-P. Seidel. Automatic photo-to-terrain alignment for the annotation of mountain pictures. In *Computer Vision and Pattern Recognition (CVPR), 2011 IEEE Conference on*, pages 41–48. IEEE, 2011.
- [2] E. S. Bradley and K. C. Clarke. Outdoor webcams as geospatial sensor networks: Challenges, issues and opportunities. *Cartography and Geographic Information Science*, 38(1):3–19, 2011.
- [3] A. Castelletti, S. Galelli, M. Restelli, and R. Soncini-Sessa. Tree-based feature selection for dimensionality reduction of large-scale control systems. In *Proceedings of the IEEE Symposium on Adaptive Dynamic Programming and Reinforcement Learning*, Paris, France, 11–15 April 2011.
- [4] S. Daume, M. Albert, and K. von Gadow. Forest monitoring and social media-complementary data sources for ecosystem surveillance? *Forest Ecology and Management*, 316:9–20, 2014.
- [5] B. De Longueville, R. S. Smith, and G. Luraschi. OMG, from here, I can see the flames!: a use case of mining location based social networks to acquire spatio-temporal data on forest fires. In *Proceedings of the 2009 international workshop on location based social networks*, pages 73–80. ACM, 2009.
- [6] Q. Desreumaux, P. Côté, and R. Leconte. Role of hydrologic information in stochastic dynamic programming: a case study of the Kemano hydropower system in British Columbia. *Canadian Journal of Civil Engineering*, 41(9):839–844, 2014.
- [7] A. J. Dietz, C. Kuenzer, U. Gessner, and S. Dech. Remote sensing of snow—a review of available methods. *International Journal of Remote Sensing*, 33(13):4094–4134, 2012.
- [8] R. Fedorov, A. Camerada, P. Fraternali, and M. Tagliasacchi. Estimating snow cover from publicly available images. *IEEE Transactions on Multimedia*, 18(6):1187–1200, 2016.
- [9] R. Fedorov, P. Fraternali, and M. Tagliasacchi. Mountain peak identification in visual content based on coarse digital elevation models. In *Proceedings of the 3rd ACM International Workshop on Multimedia Analysis for Ecological Data*, pages 7–11. ACM, 2014.
- [10] W. E. Forum. Global risks 2015 report (10th edition).
- [11] S. Galelli, G. Humphrey, H. Maier, and et al. An evaluation framework for input variable selection algorithms for environmental data-driven models. *Environmental Modelling & Software*, 62:33–51, 2014.
- [12] P. Geurts, D. Ernst, and L. Wehenkel. Extremely randomized trees. *Machine Learning*, 63(1):3–42, 2006.
- [13] M. Giuliani, A. Castelletti, F. Pianosi, E. Mason, and P. Reed. Curses, tradeoffs, and scalable management: advancing evolutionary multi-objective direct policy search to improve water reservoir operations. *Journal of Water Resources Planning and Management*, 142(2), 2016.
- [14] M. Giuliani, F. Pianosi, and A. Castelletti. Making the most of data: an information selection and assessment framework to improve water systems operations. *Water Resources Research*, 51(11):9073–9093, 2015.
- [15] D. Hadka and P. Reed. Borg: An Auto-Adaptive Many-Objective Evolutionary Computing Framework. *Evolutionary Computation*, 21(2):231–259, 2013.
- [16] M. Hejazi, X. Cai, and B. Ruddell. The role of hydrologic information in reservoir operation—learning from historical releases. *Advances in Water Resources*, 31(12):1636–1650, 2008.
- [17] H. Maier, Z. Kapelan, J. Kasprzyk, and et al. Evolutionary algorithms and other metaheuristics in water resources: Current status, research challenges and future directions. *Environmental Modelling & Software*, 62(0):271–299, 2014.
- [18] N. Michelsen, H. Dirks, S. Schulz, S. Kempe, M. Al-Saud, and C. SchÄijth. Youtube as a crowd-generated water level archive. *Science of the Total Environment*, 568:189–195, 2016.
- [19] D. Rüfenacht, M. Brown, J. Beutel, and S. Süsstrunk. Temporally consistent snow cover estimation from noisy, irregularly sampled measurements. In *Proc. 9th International Conference on Computer Vision Theory and Applications (VISAPP)*, 2014.
- [20] R. Salvatori, P. Plini, M. Giusto, and et al. Snow cover monitoring with images from digital camera systems. *Italian Journal of Remote Sensing*, 43:137–145, 2011.
- [21] S. Shukla, N. Voisin, and D. P. Lettenmaier. Value of medium range weather forecasts in the improvement of seasonal hydrologic prediction skill. *Hydrol. Earth Syst. Sci. Discuss.*, 9(2):1827–1857, 2012.
- [22] J. Tejada-Guibert, S. Johnson, and J. Stedinger. The value of hydrologic information in stochastic dynamic programming models of a multireservoir system. *Water Resources Research*, 31(10):2571–2579, 1995.
- [23] F. Yokota and K. Thompson. Value of information analysis in environmental health risk management decisions: past, present, and future. *Risk analysis*, 24(3):635–650, 2004.
- [24] J.-Y. You and X. Cai. Determining forecast and decision horizons for reservoir operations under hedging policies. *Water resources research*, 44(11), 2008.
- [25] H. Zhang, M. Korayem, D. J. Crandall, and G. LeBuhn. Mining photo-sharing websites to study ecological phenomena. In *Proceedings of the 21st international conference on World Wide Web*, pages 749–758. ACM, 2012.